File: {Books}4480-Wandas Pageproofs/3d/0444518495-ch015.3d
Creator: saravanan/cipl-u1-3b2-10.unit1.cepha.net Date/Time: 19.11.2004/3:47pm Page: 285/292

Gas hydrate dissociation and sea floor collapse in the wake of the Storegga Slide, Norway

Christian Berndt, Jürgen Mienert, Maarten Vanneste and Stefan Bünz

Two-dimensional seismic data from the Mid-Norwegian margin provide evidence for sediment liquefaction and fluid mobilisation within the sediments that were located at the base of the hydrate stability zone before the Storegga Slide occurred. The disturbed subsurface sediments are overlain by a prominent roll-over structure and sea floor collapse. This indicates fluid escape from the formerly hydrated sediment and suggests that the landslide caused a pressure drop strong enough to dissociate the gas hydrates. We calculate that this fluid escape must have taken place within less than 250 years after the slide, as the effect of pressure decrease on hydrate stability was later compensated by a temperature decrease, related to the slumping process. The volume of expelled fluids from the collapse structure exceeds the volume of the gas hydrate dissociation products, implying that gas hydrate dissociation significantly affected the surrounding sediments.

Introduction

Natural gas hydrates are clathrates of light hydrocarbons, such as the greenhouse gas methane, which are captured in water-ice crystals. They occur under pressure/temperature conditions frequently encountered in ocean sediments at water depths greater than 500 m. Kvenvolden (1993) estimated that gas hydrates bound more than half of the Earth's carbon that could potentially influence climate. Therefore, it is necessary to assess the mobility of this reservoir. So far, evidence for natural gas hydrate dissociation is sparse and most of the reported examples are from settings in which gas hydrates dissociate slowly, as for example in areas of rapid sedimentation (Dillon et al., 1998; Milkov, 2000), tectonic uplift (von Huene and Pecher, 1999) or ocean warming (Mienert et al., 2001). Here, we present geophysical evidence from the hydrated sediments of the Norwegian Margin (Fig. 1) that gas hydrates have decomposed and released fluids adjacent to the side wall rapidly after the Storegga Slide event. Fast fluid escape is a prerequisite for rapid impact of gas hydrate dissociation on climate, and may support the 'clathrate gun hypothesis' (Kennett et al., 2003).

Geological background

The Mid Norwegian margin is a passive continental margin that developed during the continental break-up between Fennoscandia and Laurentia, 54 Ma ago (Saunders et al., 1997). The two top-most sedimentary formations relevant for this study include the Miocene/earliest Pliocene Kai Formation and the Plio-/Pleistocene Naust Formation (Dalland et al., 1988; Rokoengen et al., 1995). The Kai Formation is generally characterised by fine-grained hemipelagic oozes. The overlying Naust formation is characterised by pronounced changes in lithology. It encompasses sediments of the Plio-/Pleistocene glacial–interglacial cycles consisting of debris flow deposits and hemipelagic sediments, respectively. The main depocentres of the glacigenic deposits are located along the shelf break in front of glacial trough-mouth fans (Dahlgren et al., 2002; Henriksen and Vorren, 1996; Vorren et al., 1998). Sediments deposited at the shelf break were remobilised and transported mostly downslope, as the debris flows. Contour currents sustained high sedimentation rates in the basin during deglaciation and interglacials (Laberg et al., 2001). The resulting hemipelagic contourite drift deposits

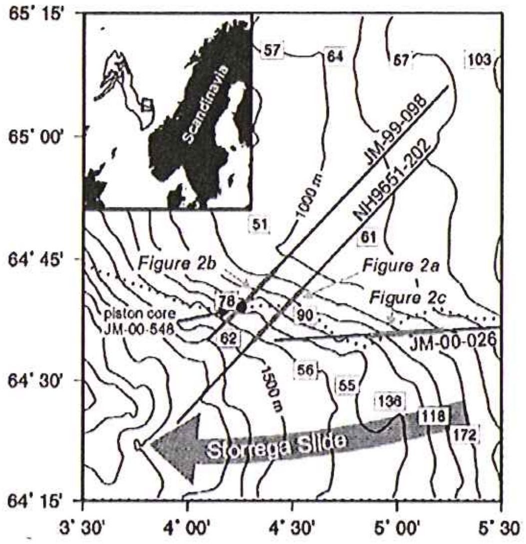

Fig. 1 Study area at the northern rim of the Storegga Slide. Gray lines indicate seismic profiles shown in Fig. 2. Numbers in boxes indicate heat flow measurements in mW/m^2 after Sundvor et al., 2000. Dotted line, boundary of the Storegga Slide; VB, Vøring Basin, MB, Møre Basin.

frequently interlayer the glacigenic debris flow deposits (Bryn et al., 2003).

One of the largest known submarine slides on the continental margins, the Storegga Slide (Fig. 1), cuts deep into the sediments of the Naust Formation of the Møre Basin (Bugge et al., 1987). This submarine slide had a maximum run-out from the shelf break to the abyssal plain of 800 km. The eastern headwall reaches up to 300 m in height and extends for about 300 km from north to south, along the shelf break. The northern sidewall is up to 100 m high and runs roughly in east-west direction along the border between the Vøring and the Møre Basins (Fig. 1). The submarine landslide transported approximately 3400 km^3 of sediments (Bryn et al., 2003), and occurred in up to 9 phases, which took place within a very short period of time at ~8.2 calendar ka B.P. (Bryn et al., 2003). The triggering mechanism is possibly a combination of various effects, e.g. earthquakes and gas hydrate dissociation. (Bugge et al., 1987) and (Mienert et al., 2002) suggested that gas hydrate dissociation contributed to slope instability as there is a bottom-simulating reflector (BSR) in an area of ~4000 km^2 in water depth of 550–1300 m (Bünz et al., 2003). The BSR is shallowest with 860 ms two-way travel time (twt) beneath sea surface (180 ms twt sub-bottom depth) in the vicinity of the headwall, and deepest with 2150 ms twt (385 ms twt sub-bottom depth) at the northern sidewall. On the continental slope, the lithology of glacigenic debris flow deposits and pre-glacial basin deposits of the Kai Formation prevent gas hydrate formation, because of reduced pore size, reduced water content and fine-grained sediment composition (Bünz et al., 2003). Towards the continental shelf, the shoaling and the pinch out of the gas hydrate stability zone terminates the area of gas hydrate growth.

Observations

In this study, we use two seismic reflection data sets. The 96-channel data (Fig. 2a) are provided by Norsk Hydro ASA, whereas we acquired the single-channel data (Fig. 2b and c) in 1999 and 2000, during the R/V Jan Mayen cruises. Both the data sets image the top 500 m of the sediment with high resolution, as the sleeve gun sources generated seismic signals with frequency bands from 10 to 130 and from 50 to 250 Hz, respectively. Both surveys have been processed including Stolt migration.

The high-resolution seismic reflection data show a distinct roll-over structure that is most pronounced towards a normal fault that coincides with the 110 m-high side wall of the submarine Storegga Slide (Fig. 2a and b). The roll-over involves the upper 150 ms twt of the seismic section, whereas the underlying strata are undisturbed. The throw of the fault is of the order of 60 ms twt or approximately 50 m. The seismic character of the strata directly above the Top Kai reflector (Fig. 2) at approximately 2.15 s twt is chaotic, and this chaotic seismic facies continues between 3 and 10 km downslope of the slide scarp. Beyond this zone the seismic reflectors are undisturbed. The depth of the base of this chaotic facies and the top of the undisturbed reflections coincide with the depth of a BSR observed outside the slide area, which has been attributed to gas accumulation beneath gas hydrates (Mienert et al., 1998). Whereas the chaotic facies coincides with the laterally projected BSR on some lines (Fig. 2a), it is located above the BSR on others (Fig. 2b). However, if it is above the projected BSR, the top of the Kai Formation bounds it at its base. Locally, a BSR is visible within the slide area (Fig. 2c; Bouriak et al., 2000).

The area of the collapse structure varies along the slide side wall between 7475 and 183 000 m^2 (Fig. 3). The area of collapse along individual transects is given in Table 1. However, the values for lines SG9801-305, SG9801-114 and JM00-010 must be considered as not representative,

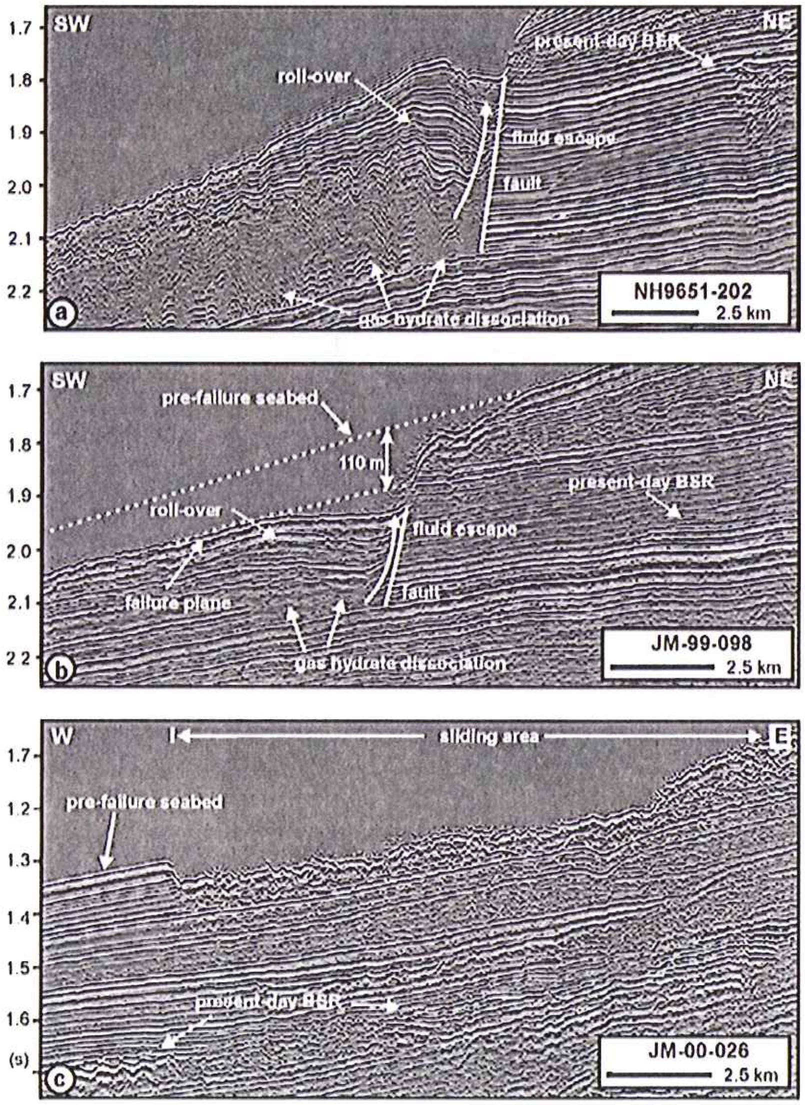

Fig. 2 Migrated high-resolution seismic data. (a) multi-channel data. (b and c) single-channel data. Note, that the bottom simulating reflector (BSR) within the slide area (c) mimicks the sea floor indicating that it has adapted to the new pressure/temperature conditions.

because the lines strike parallel to the collapse feature. Therefore the typical area of collapse in any given seismic cross-section across the collapse structure is between 7475 and 56818 m^2.

Discussion

Evidence for subsurface mass movement

The fact that the strata underlying the roll-over structure remain undisturbed (Fig. 2a and b) implies that mass has been transported away from the base of the roll-over structure. Subsurface transport of mass in a direction perpendicular to the seismic lines must have been minor, because all parallel lines show a lack of material at the base of the fault. Therefore, we conclude that most of the missing mass must have escaped to the surface. The most likely conduit for this transport is along the fault as there is no seismic evidence for other transport mechanisms, such as mud diapirs. This does not exclude, however, that the intensity of fluid flow might have varied along the collapse structure. We interpret the chaotic seismic facies between the base of the roll-over structure and the

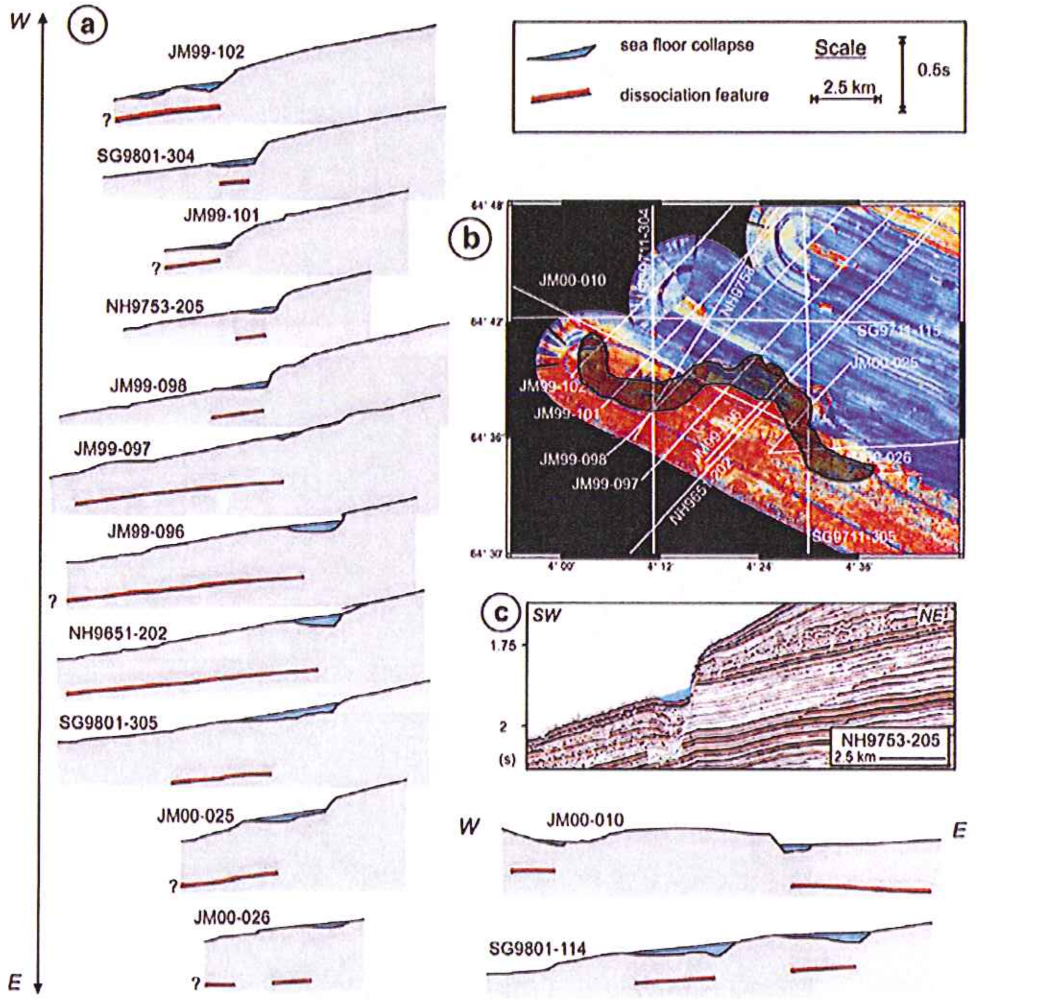

Fig. 3 (a) Geometry and size of sediment disturbance and the associated sea floor collapse structure for all seismic transects. Numerical estimates for the areas, lengths, and computed volumes are given in Table 1. (b) Side-scan sonar imagery of the slide area with sea floor collapse in dark grey, red colors — high backscatter, blue colors — little backscatter. (c) seismic type example.

Table 1 Areas of sea floor collapse and gas hydrate dissociation. Dissociation length, length of observed chaotic zone in the seismic data; Dissociation area, product of dissociation length and 8 m.

Seismic Line	Collapse area (m^2)	Dissociation length (m)	Dissociation area (assuming 8 m) (m^2)	Ratio (%)
JM99-102	35 100 + 40 000 = 75 100	min. 4700	min. 37 600	max. 199
SG9801-304	31 800	1200	9 600	331
JM99-101	7 475	min. 2560	min. 20 480	max. 36
NH9753-205	14 150	1200	9 600	147
JM99-098	19 550	2670	21 360	91
JM99-097	8 200 + 5000 = 13200	7740	61 920	21
JM99-096	43 680	min. 9800	min. 78 400	max. 58
NH9651-202	45 500	min. 6900	min. 55 200	max. 82
SG9801-305	11 4000	560 + 2600 = 3160	25 300	450 (striking the collapse structure)
JM00-025	56 818	min. 5400	min. 43 200	max. 131
JM00-026	21 400	1900 + min. 1900 = min. 3800	min. 30 800	max. 70
JM00-010	20 400 + 11 100 = 31 500	2250 + 6750 = 9000	72 000	43
SG9801-114	91 000 + 92000 = 18 3000	2800 + 3600 = 6400	51 200	357 (striking the collapse structure)
Sum	**65 7173**		**516660**	**127**

top of the undisturbed sediments to be the result of liquefaction of the sediments and mobilisation of fluids. It appears that both fault and roll-over structure, developed as the result of sediment and fluid removal from the base of the roll-over structure, as the seismic data show no indications for a pre-existing fault at this location.

Mobilisation due to gas hydrate dissociation

The extent of the disturbed sediments is confined to the vicinity of the fault and our data do not show such features farther inside the slide area. This localised disturbance would not be anticipated, if the disturbance was caused by regional, seismicity-related liquefaction. Therefore, it is more likely that a different mechanism must have caused these structures. The disturbed sediments lie at the projected depth of the pre-slide gas hydrate stability zone. This is evident from their location just above the BSR observed outside the slide area (Fig. 2a). The presence of gas hydrate-bearing sediments is commonly inferred from the presence of this characteristic reflector, which is caused by the impedance contrast between hydrated sediments and free gas that is trapped underneath (Pecher et al., 1996; Mienert et al., 2001). The coincidence of the depth of disturbed sediments and the base of the gas hydrate stability zone strongly suggests that the sediment disturbance is related to gas hydrates. On lines on which the base of the Naust Formation lies above the projected base of the gas hydrate stability zone, the chaotic zone starts not directly above the gas hydrate stability zone, but higher up at the base of the Naust Formation. We attribute this to the fact that gas hydrates only exist within the Naust Formation and not in the Kai Formation (Bünz et al., 2003). This supports the interpretation that gas hydrate dissociation causes the sediment mobilisation.

The lithostatic pressure decrease due to the Storegga Slide event ~8.2 calendar ka ago, is a possible explanation for a sudden shoaling of the gas hydrate stability zone. Increased seismic amplitudes at the base of the BSR (Fig. 2) indicate that gas is present underneath the gas hydrates. This reservoir is most likely under close to critical pressure (Flemings et al., 2003; Hornbach et al., 2004) and it is reasonable to assume that the pre-landslide conditions at the base of the gas hydrate stability zone were similar. The pore pressure decrease due to the landslide depends on the amount of this overpressure. For our argument we assume that the pore pressure drop approximately equals the difference in lithostatic pressures before and after the landslide, as close-to-critical pore pressures seem to be normal for the free gas zones under gas hydrates (Hornbach et al., 2004). A stepwise decrease in pore pressure might be an oversimplification as the pore pressure might be as low as hydrostatic pressure during the depressurisation event. However, as a result of the pressure decrease, the lowermost hydrated sediments were no longer within the stability zone. Provided that the surrounding sediments supplied enough thermal energy, the hydrates started to dissociate releasing fluids that could propagate upwards through the fault. Subsequently the geothermal field adjusted to the new conditions leveling out the temperature difference between the cold bottom-water and the newly exposed, i.e. warmer, sediments at the sea floor. The sediments progressively cooled downwards until the conductivity-controlled geothermal gradient was re-established. Gas hydrate dissociation must have stopped when the thermal signal had reached the pre-landslide depth of the gas hydrate stability zone and re-stabilized the gas hydrates. This is evidenced by the observation of a re-adjusted BSR within the slide area (Fig. 2c).

Quantification of the thermal evolution

In order to estimate the maximum time of gas hydrate dissociation, we calculate the thermal evolution of the sedimentary column since the sliding event. Because the landslide removed the overburden and, consequently, exposed the warmer, deeper material at the seabed, we assume that an instantaneous sea floor temperature change has imposed on a homogeneous conductive medium (Vanneste, 2000). This does not take into account the possible heat transport due to fluid flow. However, such heat transport will shorten the time available for dissociation because it will re-establish the thermal equilibrium faster than conductive heat transport alone. For the calculation we also assume lithostatic pressures. This might overestimate the effect of the pressure drop leading to a larger thickness of dissociating hydrates, and hence, our calculations give an upper limit. In case the pressure distribution is purely hydrostatic, removal of part of the overburden would not result in *in situ* pressure drop and hydrate would not dissociate. Given these caveats, the temperature T as a function of time t, and the sub-bottom depth z can be described by the initial conditions and a complementary error function, Erfc (Carslaw and Jaeger, 1959):

$$T(z, t) = T_0 + Gz + \Delta T Erfc\left(\frac{z}{2\sqrt{\kappa t}}\right)$$

with T_0: the pre-landslide temperature at the slide plane, G: the geothermal gradient, ΔT the temperature difference at the new sea floor exposed by the slide, and κ the average thermal diffusivity of the sediments involved. The physical sediment properties used in the calculation are based on the logging results of a piston core taken at the slide's side wall (Fig. 1) and from the seismic constraints (Table 2). The calculations indicate that the landslide initially moved the lowermost 8 m of sediment out of the pre-slide gas hydrate stability zone initiating gas hydrate dissociation within this layer (Fig. 4). After 60 years, the thermal signal reached the pre-landslide depth of the gas hydrate stability zone beginning to re-stabilise the gas hydrates at the top of the 8 m layer and 180 years after the landslide, the new base of the gas hydrate stability zone had reached pre-landslide depth. At that time, gas hydrate dissociation must have terminated. Our model predicts that re-adjustment of the geotherm still continues. Today, the base of the gas hydrate stability zone is ~80 m deeper than the pre-slide base. The error of these calculations depends mainly on the thermal diffusivity, and is on the order of 40%. The errors of the remaining parameters such as the parameters deduced from seismic interpretation and the effects of additional physical processes, such as latent heat generation, are small compared to this. This implies that fluid escape must have happened within a maximum of 180 ± 70 years after the landslide and perhaps even faster.

Implications for fluid expulsion

Because the upper limit of gas hydrate dissociation is not imaged in the seismic data due to disturbance of the sediments, it is necessary to use an indirect approach to quantify the area of dissociation, along individual seismic transects. Therefore, we mapped the length of the zone where chaotic reflectors and dissociation occurred (Fig. 3) and multiplied the length with the theoretically expected height of 8 m, assuming in the absence of a detailed information that this height is representative for the entire collapse structure. The area varies between 9600 and 78 400 m^2 for each transect (Table 1).

Comparing the areas of gas hydrate dissociation and the sea floor collapse as a proxy of how much mass was mobilised due to gas hydrate dissociation,

Table 2 Modelling Parameters.

Property	Value	Reference
Bulk density	1850 kg/m^3	Piston core JM-00-548
Bottom water temperature	0°C	Mienert et al., 1998
Thermal conductivity	1.2 W/mK	Sundvor et al., 2000
Bulk specific heat capacity	800–1300 J/kg K	Buntebarth, 1984
Geothermal gradient Outside the slide area	62 K/km	Hydrate stability conditions
Thickness of removed sediments	110 m	Seismic line JM-99-098

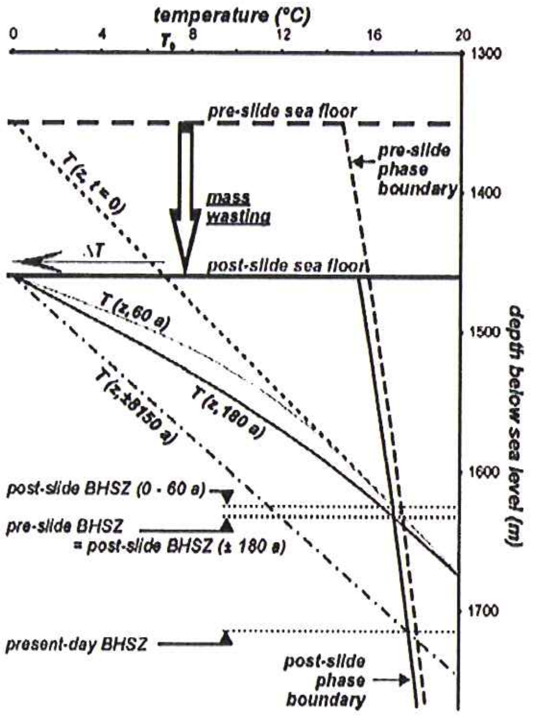

Fig. 4 Thermal evolution at the foot of the Storegga Slide side wall. Note the initial shoaling of the hydrate stability zone immediately after the occurrence of the landslide and subsequent deepening. Hydrate dissociation and fluid escape must occur within 180 +/− 70 years after the sliding event. BHSZ, base of the hydrate stability zone; T, temperature, T0, temperature difference at the sea floor due to the slides.

yields percentages between 21 and 331% (excluding the two strike lines). On an average, the collapse area is slightly bigger (127%) than the sediment layer in which dissociation has occurred (Table 1). This implies that generally fluid volumes were expelled from the sediments that were much larger than the total volume of sediments in which hydrate dissociation has happened on the basis of theoretical considerations, because hydrates constitute only a small fraction of the total sediment volume in this area (Andreassen et al., 2003). As the uncertainty of the theoretical considerations is up to 40%, this implies that fluids, in addition to those released by gas hydrate dissociation, were expelled from the subsurface. There is no evidence for sediment distortion underneath the dissociation feature (Figs. 2 and 3c), but the sediments 50–100 m above the 8 m thick basal layer of the gas hydrate stability zone are disturbed (Figs. 2 and 3c). Having this in mind, we conclude that the gas hydrate dissociation caused liquefaction of the overlying sediments within the gas hydrate stability zone, and that not only the hydrate dissociation products were expelled but also fluids and sediments from the surrounding sediments contribute to the amount of expelled fluid. As there is no obvious seismic or side scan sonar evidence of expelled sediments at the present seabed we conclude that most of the transported material was pore water and that only little sediment made its way to the surface.

Conclusions

Sea floor collapse within the Storegga Slide region and above dissolved gas hydrates shows that the gas hydrate reservoir is highly dynamic. Our calculations show that it can release fluids from the base of the hydrate stability zone to the surface within decades. This makes the release of methane due to submarine landslides a process that potentially can influence climate. However, ice core data from Greenland show that it takes very large methane input, i.e. of the order of 4000 Tg, to increase hte global mean temperatures by 0.3 to 1 K (Thorpe et al., 1998), and it is not clear whether submarine slope failures, such as the Storegga Slide events did release enough methane from the gas hydrate reservoir to the atmosphere to influence climate (Raynaud et al., 1998).

The Storegga Slide head wall extends for 300 km (Bugge et al., 1987) and has developed simultaneously (Haflidason et al., 2001). So far, it is not clear what caused the slope failure at such large regional scale. The observation of induced sea floor collapse in the wake of landslides suggests a possible propagation mechanism: an initial local slope failure, possibly induced by an earthquake, may not only have started the gas hydrate dissociation and fluid expulsion under the initial slide area but also in the adjacent parts of the slope, because the pressure drop will also effect the vicinity of the slide. A subsequent sea floor collapse and the rise of fluids perhaps, decreased the shear strength of the sedimentary overburden leading to more regional slope failure.

Acknowledgements

We thank the captains of R/V Jan Mayen and their crew for their help during data acquisition. Special thanks go to Steinar Iversen for skillfully handling and maintaining the seismic equipment. The manuscript improved through constructive input from the editor Johan Petter Nystuen and the reviewers Deborah Hutchinson, Dendy Sloan, Jr. and Martin Hovland. GMT (Wessel and Smith, 1991) was extensively used for figure preparation. This work is a contribution to the COSTA Project funded under FP5 of the European Commission EVK-CT-1999-00006 and the DFG Project MI306/10-1. Additional funding was provided by the Ormen Lange Licensing Group, contract NHT-B44-VK0768-00. Norsk Hydro ASA kindly provided seismic data presented in Fig. 2a through the COSTA-Seabed Project co-operation. Furthermore, we acknowledge support by the Landmark Graphics University Programme.

References

Andreassen, K., Berteussen, K.A., Sognnes, H., Henneberg, K., Langhammer, J. and Mienert, J., 2003. Multi-component ocean bottom cable data in gas-hydrate investigations. J. Geophys. Res., 108: 2399.

Bouriak, S., Vanneste, M. and Saoutkine, A., 2000. Inferred gas hydrates and clay diapirs near the Storegga Slide on the southern edge of the Vøring Plateau, offshore Norway. Mar. Geol., 163: 125–148.

Bryn, P., Solheim, A., Berg, K., Lien, R., Forsberg, C.F., Haflidason, H., Ottesen, D. and Rise, L., 2003. The Storegga Slide complex: Repeated large scale sliding in response to climatic cyclicity. In: J. Locat and J. Mienert (Editors), Submarine Mass Movements and their Consequences. Kluwer Academic Publishers, Kluwer, pp. 215–222.

Bugge, T., Befring, S., Belderson, R.H., Eidvin, T., Jansen, E., Kenyon, N.H., Holtedahl, H. and Sejrup, H.P., 1987. A giant three-stage submarine slide off Norway: Geo-Mar., Lett., 7: 191–198.

Bünz, S., Mienert, J. and Berndt, C., 2003. Geological controls on the Storegga gas-hydrate system of the mid-Norwegian continental margin. Earth Planet. Sci. Lett., 209: 291–307.

Buntebarth, G.,1984. Geothermics; an introduction, Springer Verlag, Berlin.

Carslaw, H.S. and Jaeger, J.C., 1959. Conduction of Heat in Solids, 2nd ed., Clarendon Press, Oxford, UK.

Dahlgren, K.I.T., Vorren, T.O. and Laberg, J.S., 2002. Late Quaternary glacial development of the mid-Norwegian margin — 65 to 68°N. Mar. Petrol. Geol., 19: 1089–1113.

Dalland, A., Worsley, D. and Ofstad, K., 1988: A lithostratigraphic scheme for the Mesozoic and Cenozoic succession offshore mid- and northern Norway. NPD Bull., 4: 65 pp.

Dillon, W.P., Danforth, W.W., Hutchinson, D.R., Drury, R.M., Taylor, M.H. and Booth, J.S., 1998. Evidence for faulting related to dissociation of gas hydrate and release of methane off the southeastern United States. In: J.-P. Henriet and J. Mienert (Editors), Gas Hydrates: Relevance to World Margin Stability and Climate Change, Geol. Soc., London, Spec. Publ., 137: 275–291.

Flemings, P.B., Liu, X. and Winters, W.J., 2003. Critical pressure and multiphase flow in Blake Ridge gas hydrates. Geology, 31: 1057–1060.

Haflidason, H., Sejrup, H.P., Bryn, P. and Lien, R., 2001. The Storegga Slide; chronology and flow mechanism, paper presented at the XI European Union of Geoscientists meeting, 8–12th Apr., Strasbourg, France.

Henriksen, T. and Vorren, T.O., 1996. Late Cenozoic sedimentation and uplift history on the mid-Norwegian continental shelf. Global Planet. Change, 12: 171–199.

Hornbach, M.J., Saffer, D.M. and Holbrook, W.S., 2004. Critically pressured free-gas reservoirs below gas-hydrate provinces. Nature, 427: 142–144.

Kennett, J.P., Cannariato, K.G., Hendy, I.L. and Behl, R.J., 2003. Methane Hydrates in Quaternary Climate Change: The Clathrate Gun Hypothesis. Am. Geophys. U., Spec. Publ. 54.

Kvenvolden, K.A., 1993. Gas hydrates as a potential energy resource; a review of their methane content. In: D.G. Howell, K. Wiese, M. Fanelli, L.L. Zink and F. Cole (Editors), The future of energy gases, U. S. Geological Survey Reston, VA, Professional Paper, pp. 555–561.

Laberg, J.S., Dahlgren, K.I.T., Vorren, T.O., Haflidason, H. and Bryn, P., 2001. Seismic analyses of Cenozoic contourite drift development in the Northern North Sea. Mar. Geophys. Res., 22: 401–416.

Mienert, J., Posewang, J. and Baumann, M., 1998. Gas hydrates along the northeastern Atlantic margin: possible hydrate-bound margin instabilities and possible release of methane. In: J.-P. Henriet and J. Mienert (Editors), Gas Hydrates: Relevance to World Margin Stability and Climate Change. Geol. Soc., London, Spec. Publ. 137: 275–291.

Mienert, J., Posewang, J., and Lukas, D., 2001. Changes in the hydrate stability zone on the Norwegian Margin and their consequence for methane and carbon releases into the ocean. In: P. Schäfer, W. Ritzrau, M. Schlüter and J. Thiede (Editors), The Northern North Atlantic: A Environment, Springer, Berlin, pp. 259–280.

Mienert, J., Berndt, C., Laberg, J.S. and Vorren, T.O., 2002. Submarine Landslides on Continental Margins. In: G. Wefer, D.S.M. Billet, D. Hebbeln, B.B. Jørgensen, M. Schlüter and T. van Weering (Editors), Ocean Margin Systems. Springer, Berlin, pp. 179–193.

Milkov, A.V., 2000. Worldwide distribution of submarine mud volcanoes and associated gas hydrates. Mar. Geol. 167: 29–42.

Pecher, I., Minshull, T.A., Singh, S.C. and von Huene, R., 1996. Velocity structure of a Bottom Simulating Reflector offshore Peru. Earth Planet. Sci. Lett., 139: 459–469.

Raynaud, D., Chappellaz, J. and Blünier, T., 1998. Ice-core data of atmospheric methane changes: relevance to climatic changes and possible gas hydrate sources. In: J.-P. Henriet and J. Mienert (Editors), Gas Hydrates: Relevance to World Margin Stability and Climate Change, Geol. Soc., London, Spec. Publ., 137: 327–331.

Rokoengen, K., Rise, L., Bryn, P., Frengstad, B., Gustavsen, B., Nygaard, E. and Sættem, J., 1995. Upper Cenozoic stratigraphy on the Mid-Norwegian continental shelf. Norsk Geol. Tidsskr., 75: 88–104.

Saunders, A.D., Fitton, J.G., Kerr, A.C., Norry, M.J. and Kent, R.W., 1997. The North Atlantic Igneous Province. In: J.J. Mahoney and M.F. Coffin (Editors), Large Igneous Provinces: Continental, Oceanic, and Planetary Flood Basalt Volcanism. Am. Geophys. U., Geophys. Monograph., pp. 45–93.

Sundvor, E., Eldholm, O., Gladczenko, T. and Planke, S., 2000. Norwegian-Greenland Sea thermal field. In: A. Nøttvedt (Editor), Dynamics of the Norwegian Margin, Geol. Soc., London, Spec. Publ., 176: 397–410.

Thorpe, R.B., Pyle, J.A. and Nisbet, E.G., 1998. What does the ice-core record imply concerning the maximum climatic impact of possible gas hydrate release at Termination 1A? In: J.-P. Henriet and J. Mienert, (Editors), Gas Hydrates: Relevance to World Margin Stability and Climate Change, Geol. Soc., London, Spec. Publ., 137: 319–326.

Vanneste, M., 2000. Gas hydrate stability and destabilisation processes in lacustrine and marine environments: Results from theoretical analyses and multi-frequency seismic investigations, Ph.D. thesis, University of Ghent, Ghent, Belgium.

Vorren, T.O., Laberg, J.S., Blaume, F., Dowdeswell, J.A., Kenyon, N.H., Mienert, J., Rumohr, J. and Werner, F., 1998. The Norwegian-Greenland Sea continental margins: Morphology and late Quarternary sedimentary processes and environment. Quaternary Sci. Rev., 17: 273–302.

von Huene, R. and Pecher, I., 1999. Vertical tectonics and the origins of BSRs along the Peru margin. Earth Planet. Sci. Lett., 166: 47–55.

Wessel, P. and Smith, W.H.F., 1991. Free software helps map and display data. EOS, 72: 441, 445–446.